JCAMECH

Vol. 51, No. 2, December 2020, pp 288-293
DOI: 10.22059/jcamech.2018.263253.309

Mechanical properties of CNT reinforced nano-cellular polymeric nanocomposite foams

Mohammad Babadi [a], *Saeed Momeni Bashusqeh* [b,*]

[a] *Faculty of Mechanical Engineering, K.N.Toosi University of Technology, Tehran, Iran*
[b] *School of Mechanical Engineering, College of Engineering, University of Tehran, Tehran, Iran*

ARTICLE INFO

Article history:
Received: 3 August 2018
Accepted: 6 October 2018

Keywords:
PMMA
Foam
Molecular dynamics
Uniaxial stretching
Dynamic compression

ABSTRACT

Mechanics of CNT-reinforced nano-cellular PMMA nanocomposites are investigated using coarse-grained molecular dynamics simulations. Firstly, static uniaxial stretching of bulk PMMA polymer is simulated and the results are compared with literature. Then, nano-cellular foams with different relative densities are constructed and subjected to static uniaxial stretching and obtained stress-strain curves are used to compute Young moduli and tensile strength of PMMA foams. Carbon nanotubes in various weight fractions and random orientations are then introduced into the constructed samples to investigate effect of reinforcement on mechanical properties of bulk and foam samples. Also dynamic compression experiment at high strain-rate is simulated in all of the samples to check effects of relative density and reinforcement on energy absorption capability and plateau stress. By plotting variation of lateral strain with respect to longitudinal strain, auxeticity of the foams at the early stage of loading was observed. It is shown that there are multiple distinct regimes in stress-strain curves obtained from simulation of compression due to densification of foams during compression. Both recoverable and unrecoverable energies per unit volume in all of the compression experiments are computed and it is shown that reinforcement of foams could result in a lighter structure with improved energy absorption.

1. Introduction

Currently, polymeric foams have attracted considerable attention in various applications e.g. in the automotive, construction, aerospace because of their lightweight, and good thermal and acoustic insulation capabilities. However, polymer foams have shown lower mechanical properties than their bulk counterparts [1, 2] which makes it vital to find a solution to overcome this shortcoming. Carbon nanotubes (CNT) have demonstrated to have improved structural, mechanical and electrical properties when compared to typical carbon fillers. So it is of great priority to investigate effect of CNT reinforcement on mechanical properties of polymeric foams and see if it is possible to obtain a polymeric foam structure with improved mechanical properties. CNTs are being widely used as fillers because of the exceptional stiffness and strength, and remarkable high aspect ratio and electrical properties [3]. Improvement of polymeric foam properties by means of CNTs is a solution to create strong and lightweight material. Beside the mechanical strength, energy dissipation is becoming an important feature in today's industries. This feature deals with a materials ability to withstand impact and act as a barrier against negative forces. Research involving energy dissipation or energy absorption is important because it affects many areas of everyday life.

There have been extensive efforts to study mechanical properties of reinforced polymer composites both experimentally and theoretically [4-8]. It is known that experimental studies are not capable of providing clear insight into processes at molecular scale. Instead, Molecular dynamics (MD) simulations can provide us with detailed information at nanoscale. Given a lower computational cost, coarse-grained molecular dynamics models are now being used widely in computational material sciences [9]. In coarse-grained models, certain atoms are grouped in new interaction sites which results in lower degrees of freedom and hence computational cost. Arash et. al. [10] proposed a coarse-grained model to express interactions between different beads in CNT reinforced PMMA nanocomposites. Using this model, they studied behavior of short CNT reinforced polymer composite subjected to tensile loading [11]. The effects of the CNT weight fraction and their length-to-diameter aspect ratio on mechanical properties of the polymer composite were studied. Also a simulation method was proposed based on their CG model to

* Corresponding author. Tel.: +98-935-671-7721; e-mail: s.momeni@ut.ac.ir

calculate J-integral of reinforced polymer composites [12].Following a similar approach proposed by Arash et. al. [10], a CG model was proposed for studying mechanical properties of cross linked short carbon nanotube/polymer composites [13]. Temperature dependent mechanical properties of grapheme reinforced polymer nanocomposites was studied Lin et. al. [14]. They employed molecular dynamics method to simulate grapheme reinforced polymer composite under mechanical loads in various levels of reinforcement and temperatures. They could demonstrate temperature dependency of mechanical properties of grapheme reinforced polymer composite. Combining dissipative particle dynamics method and continuum mechanics based finite element method, Lin et. al. [15] studied morphological and mechanical properties of grapheme reinforced PMMA nanocomposites. Also, molecular dynamics method was employed to study glass transition temperature and thermal diffusivity of PMMA/modified alumina nanocomposites [16-17]. To do this, variation of density with temperature was obtained and the temperate at which slope of the variation changes dramatically was regarded as glass transition temperature. Alian et. al. [18] used molecular dynamics method to investigate mechanical properties of grapheme reinforced multilayered polymer nanocomposites. For this aim, they simulated nanoindentation experiment in constructed molecular samples and showed that orientation and dispersion of grapheme sheets affect mechanical properties of polymer nanocomposites significantly. Tensile behavior of polymer nanocomposites reinforced with graphene containing defects was studied by Sun et. al. using molecular dynamics method [19]. Single and double vacancies was introduced into the grapheme sheets and was shown that single vacancy is more effective on mechanical properties of polymer nanocomposites when compared to double vacancy. Molecular dynamics was also employed by Shen et. al. [20] to study mechanical and viscoelastic properties of polymer grafted nanorod composites. The nanorod/polymer interfacial properties were shown to have the main role in mechanical reinforcement efficiency. There are few works which dealt with properties of metallic foams [21-25] but mechanical properties of CNT reinforced polymeric foams have not been studied yet completely.

To the best knowledge of authors, this is for the first time that mechanical properties of CNT-reinforced polymeric foams are studied in detail using molecular dynamics method. In the current study, mechanical properties of CNT reinforced nano-cellular PMMA composites are investigated using coarse-grained molecular dynamics simulations. To do this, bulk and nano-cellular polymeric samples with and without reinforcement are constructed and then subjected to various types of mechanical loads. Stress-strain curves are obtained and used to compute mechanical properties of the samples like Young modulus and energy absorption capability. It is shown that reinforcement of polymeric foams could result in a lighter structure with improved energy absorption. Doing experiments are basically costly and laborious, so the method followed in this work can be regarded as an alternative to experimental methods and can provide researchers with deeper insight into mechanics of reinforced polymeric foams.

2. Modeling and Mechanical Properties of PMMA Foams

To construct PMMA foams, specific amount of PMMA beads are placed randomly inside the simulation box containing the bulk polymer from previous section. Attractive potentials between these new beads and PMMA beads are turned-off while the new beads can attract each other (cut-off radius for the interaction is set equal to the distance at which minimum potential energy occurs). The system is then equilibrated at ambient conditions for 10 ns. After equilibration, a two-phase structure is obtained as is shown in Fig.3. Then, recently added beads are removed and the resulting system is again equilibrated at ambient conditions. As whole the process is random, cavities with random orientations and volumes are created. By varying amount of added beads, relative density of the foam could be tuned. We added 5000 and 10000 beads which resulted in foams with relative densities of 0.749 and 0.586 denoted as Case I and Case II foams respectively. A sample RVE of the foam Case II is shown in Fig. 4.

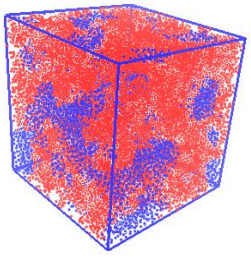

Fig.3. Two phase polymer structure polymer beads are shown with red color where the blue color beads are those would be removed.

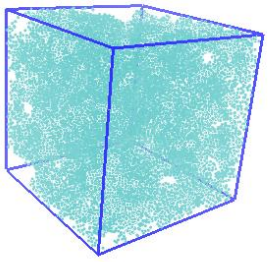

Fig.4. The foam with relative density of 0.586 (Case II)

Calculation of stress components is a challenging task in molecular dynamics simulations. Specifically in LAMMPS, computed stress for an atom is in units of pressure×volume; It would need to be divided by a per-atom volume to have units of stress (pressure), but an individual atom's volume is not a well-defined property or easy to compute. There is a method namely Voronoi Tessellation [30] to compute volume of an atom in molecular simulations but in case of cellular structures, the computed volume for atoms in vicinity of cavities is not accurate. To resolve this issue, volume of the atoms in vicinity of cavities was considered equal to average of volumes of innermost atoms. Constructing the nano-cellular structures, uniaxial stretching of these samples is simulated and the results are given below in Fig.5 where Young moduli of these structures are obtained as 1.665 GPa and 1.337 GPa.

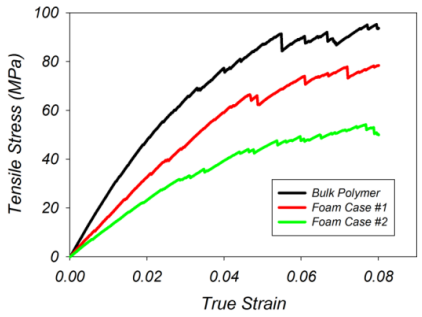

Fig. 5. Static stress-strain curves (bulk and foams)

Reducing the density of the polymer by 25.1% and 41.4%, Young modulus decreased by 41.8% and 53.2%, respectively. Also tensile strength of the foams obtained as 75.65 MPa and 52.46 MPa which shows 12% and 39% decrease when compared

to the bulk polymer, respectively. In Fig.6 stress-strain curve obtained from simulation of dynamic compression is provided. Unlike the bulk polymer, compressive stresses in foams increase with compressive strain constantly. As the foam is compressed, more beads are come to interact resulting in increasing compressive stress (more atoms are placed inside the cut-off radius of an atom). Three and two regimes could be distinguished in stress-strain curves obtained from compression of foams Case I and Case II, respectively. In foam case I, slope of the curve decreases by transition from the first regime to the second one. Another transition occurs at almost 70% compressive strain, after which slope of the curves becomes zero and magnitude of compressive stress becomes equal to magnitude of plateau stress in bulk polymer. The increase of compressive stress in foams is due to densification; therefore compressing the foam case I more than 70% has not resulted in denser polymer. In the foam Case II, increasing trend of compressive stress is seen even at 80% compressive strain which is due to being more porous in comparison to Case I. Also the modulus of resilience and unrecoverable energy per unit volume for the foams are computed and given in Table 2.

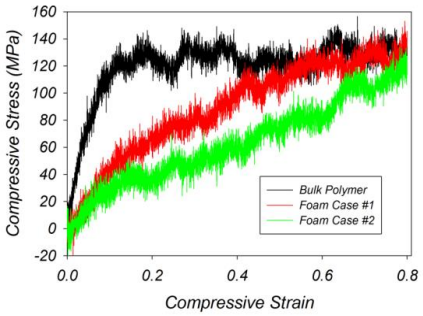

Fig. 6. Dynamic stress-strain curve (bulk and foams)

The modulus of resilience of the foams case I and II decrease by 81% and 91%, respectively. On the other hand unrecoverable energy per unit volume of the cases I and II decreases by 24.5% and 46.6%, respectively.

Table 2. Energy absorption and dissipation in PMMA Foams
Recoverable and unrecoverable energies per unit volume (Foams Case #1 and #2)

Foam Case I		Foam Case II	
Recoverable energy (J/cm^3)	Unrecoverable energy(J/cm^3)	Recoverable energy(J/cm^3)	Unrecoverable energy(J/cm^3)
0.2525	70.6884	0.1261	49.9893

Investigation of Poisson's ratio of the foam has been also considered. In this regard, variation of lateral strain with respect to longitudinal one during the compression is shown in Fig.7. This variation in bulk polymer is linear whereas in foams, lateral strain decreases with longitudinal strain at the early stage of loading and then follows an increasing trend. Rate of decrease is porosity-dependent and in case II is stronger than case I. Slope of the variation in bulk polymer gives Poisson ratio which is equal to almost 0.5. Poisson's ratio of PMMA polymer is known to be in the range of 0.35 to 0.4. The discrepancy between the computed Poisson's ratio and the reported results could be because of very high strain-rate loading of the polymer in this study. As said above, lateral dimensions of the foams are decreased upon decrease in longitudinal one which results in negative Poisson's ratio at early stage of loading. Such behavior could be found in materials with negative Poisson's ratio called Auxetic [31]. Re-entrant polymer foams were the first group in which auxeticity was reported but soon after it was shown that auxeticity is a common feature of honeycomb structures and networks [31].

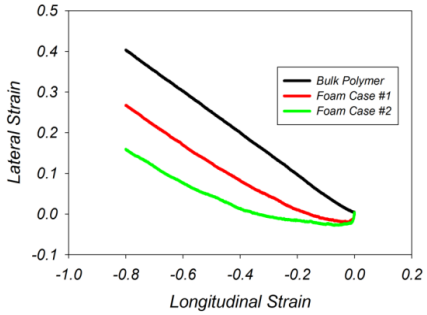

Fig.7. Variation of lateral strain with respect to longitudinal strain

In Fig. 8, the foam case #2 is shown at the end of compressive loading.

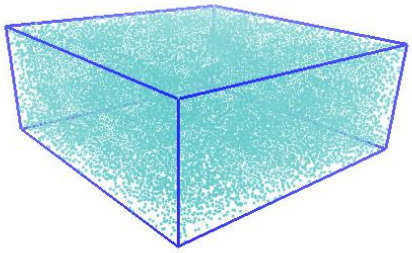

Fig. 8. Compressed foam

3. Mechanical Properties of CNT reinforced bulk PMMA polymer

Up to now, mechanical properties of bulk and cellular PMMA polymers have been investigated. The main disadvantage of foam structures is that their mechanical strength is lower than bulk counterparts as was shown in previous section. To overcome this shortcoming, carbon nanotubes can be introduced into the foams resulting in a structure with desired mechanical strength and lower mass density. To study mechanical behavior of CNT reinforced polymer, carbon nanotubes are inserted randomly into the bulk PMMA polymer prepared in section 1. Length of the nanotubes is set to 6 nm; longer nanotubes would result in higher mechanical strength [10]. Weight fractions of nanotubes are set to 1.2%, 5.6% and 12.5%. After randomly dispersion of nanotubes inside the simulation box, the system is equilibrated at 298 K and 1 atm for 10 ns. In Fig.9, dispersion of carbon nanotubes in bulk polymer is shown.

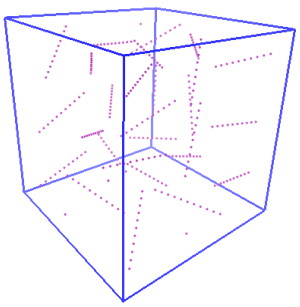

Fig. 9. Randomly dispersed nanotubes

Before applying mechanical loads (static tension and dynamic compression), total energy of the system is minimized to remove unwanted internal stresses. Using the procedures explained in previous sections, static stretching and dynamic compression in CNT reinforced bulk polymers are simulated and the results are

given in Figs. 10 and 11. Improvement of mechanical strength upon reinforcing is obvious in these curves.

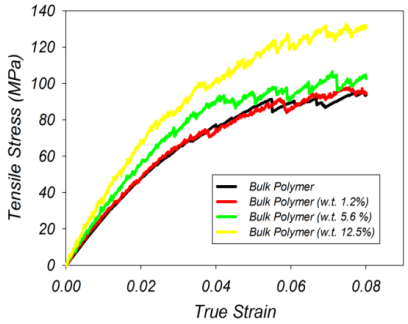

Fig. 10. Static stress-strain curve (CNT reinforced polymers)

Fitting polynomials on static stress-strain curves, Young moduli of CNT reinforced polymers are computed as tabulated in Table 3.

Table 3. Young moduli of CNT reinforced polymers

Reinforced PMMA (w.t. 1.2%)	2.946 GPa
Reinforced PMMA (w.t. 5.6%)	3.393 GPa
Reinforced PMMA (w.t. 12.5%)	4.446 GPa

Also tensile strengths of reinforced polymers are obtained as given in Table 4.

Table 4. Tensile strength of CNT reinforced polymers

Reinforced PMMA (w.t. 1.2%)	91.43 MPa
Reinforced PMMA (w.t. 5.6%)	96.93 MPa
Reinforced PMMA (w.t. 12.5%)	125.53 MPa

As was explained in section 1, compressive stress remains constant by crossing the plateau point but in case of reinforced polymers, compressive stress increases slightly in this regime. Rate of increase depends on degree of reinforcement as seen in Fig. 11.

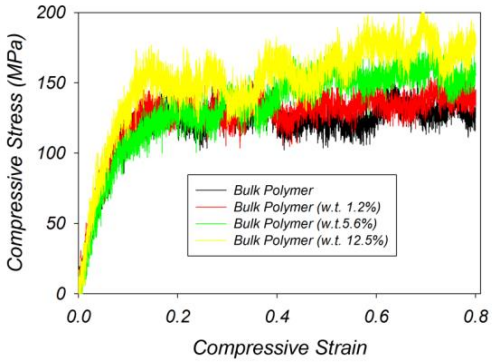

Fig. 11. Dynamic stress-strain curve (CNT reinforced polymers)

In Table 5, both recoverable and unrecoverable energies per unit volume in reinforced polymers are given as follows:

Table 5. Recoverable and unrecoverable energies per unit volume (Reinforced polymers)

Weight fraction of CNT	Recoverable energy per unit volume	Unrecoverable energy per unit volume
1.2 %	1.6334J/cm3	98.5309J/cm3
5.6 %	1.1839 J/cm3	104.7677 J/cm3
12.5 %	1.5740J/cm3	118.8960J/cm3

As it is obvious from Table 5, energy absorption capability of the polymer is improved by reinforcement.

4. Mechanical Properties of CNT reinforced PMMA foams

In order to investigate behavior of CNT reinforced PMMA foams, the Like the previous section CNTs are inserted into the foams at random positions with random orientations. Mechanical loads (static stretching and dynamic compression) are then applied on the reinforced foams after equilibration of the system and the obtained results are provided in Figs. 12-14. Using Fig.12, Young moduli of CNT reinforced foams are computed and given in Table 6:

Table 6. Young moduli of CNT reinforced foams

Foam Case #1 (w.t. 1.2%)	2.312 GPa
Foam Case #1 (w.t. 5.6%)	2.521 GPa
Foam Case #1 (w.t. 12.5%)	3.446 GPa
Foam Case #2 (w.t. 5.6%)	2.094 GPa

In section 2, Young modulus of the foam case #1 was obtained 1.665 GPa. By reinforcing (as in Table 2), Young modulus increased by 38.85%, 51.41% and 106.96%. Although Young modulus was improved considerably by reinforcement, tensile strength didn't show improvement as significantly as Young modulus. To gain clearer insight, stress-strain curves of reinforced foams case #1 along with the foam itself is shown in Fig. 13.

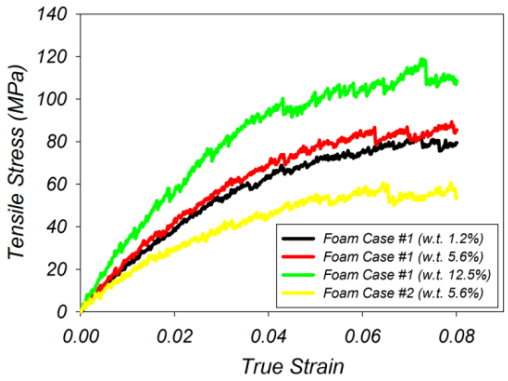

Fig. 12. Static stress-strain curve (CNT reinforced foams)

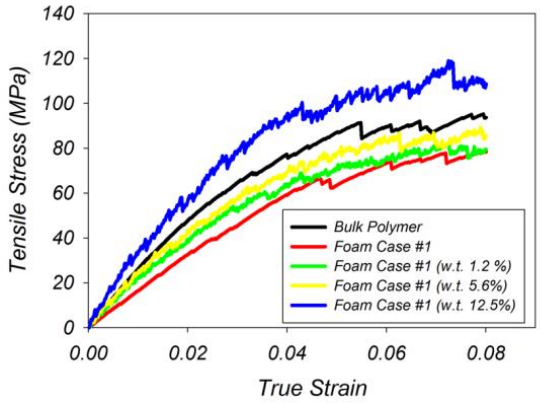

Fig. 13. Static stress-strain curves (pure and reinforced foam case #1)

As it is shown in Fig. 13, 12.5% reinforcement could result in a cellular structure stronger than its bulk counterpart. Tensile strengths of reinforced foams are tabulated in Table 7.

Table 7. Tensile strength of CNT reinforced foams

Foam Case #1 (w.t. 1.2%)	80.08 MPa
Foam Case #1 (w.t. 5.6%)	84.28 MPa
Foam Case #1 (w.t. 12.5%)	108.84 MPa
Foam Case #2 (w.t. 5.6%)	57.46MPa

In Fig. 14, stress-strain curves from dynamic compression of CNT reinforced foams are plotted. In Fig. 6, it was shown that variations of compressive stress in foams follow increasing trends with nearly constant slope in plateau regime. Reinforcing the foams, compressive stress is seen to increase with different slopes after the plateau point.

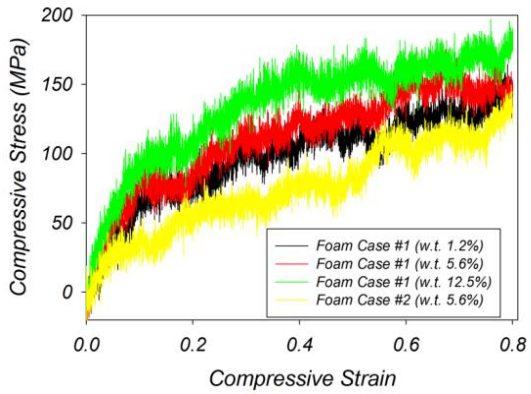

Fig. 14. Dynamic stress-strain curve (CNT reinforced foams)

In Table 8, recoverable and unrecoverable energies per unit volume in reinforced foams are provided.

Table 8. Recoverable and unrecoverable energies per unit volume (Reinforced foams)

Foam case #1-w.t. 1.2% (recoverable energy per unit volume)	0.4144J/cm^3
Foam case #1-w.t. 1.2% (unrecoverable energy per unit volume)	77.4516J/cm^3
Foam case #1-w.t. 5.6% (recoverable energy per unit volume)	0.6286J/cm^3
Foam case #1-w.t. 5.6% (unrecoverable energy per unit volume)	87.9376 J/cm^3
Foam case #1-w.t. 12.5% (recoverable energy per unit volume)	1.3421J/cm^3
Foam case #1-w.t. 12.5% (unrecoverable energy per unit volume)	105.8928J/cm^3
Foam case #2-w.t. 5.6% (recoverable energy per unit volume)	0.3584J/cm^3
Foam case #2-w.t. 5.6% (unrecoverable energy per unit volume)	59.3162 J/cm^3

12.5% reinforcement of the foam case #1 could result in a lighter structure with better energy absorption capability.

Conclusions

Mechanical properties of CNT reinforced bulk and nano-cellular PMMA polymer were studied using coarse-grain molecular dynamics simulations. Firstly, static stretching experiment in bulk PMMA polymer was simulated and the results were compared to published results. Then dynamic compression of the polymer at high strain rate was simulated and it was shown that compressive strain does not vary much after crossing the plateau strain. Nano-cellular structures were then constructed following a straightforward approach resulting in cavities with random volumes and orientations inside the bulk sample. Reduced strength of foams was justified and it was shown that there are multiple distinct regimes in stress-strain curves obtained from simulation of compression due to densification of foams during compression. By plotting variation of lateral strain with respect to longitudinal strain, auxeticity of the foams at the early stage of loading was observed. Inserting carbon nanotubes at random positions with random orientation, CNT reinforced bulk polymers were loaded both statically (stretching) and dynamically (compression). Improvement of mechanical strength of the polymer upon reinforcing was shown and it was illustrated that compressive stress in reinforced samples follows a slightly increasing trend (which depends on degree of reinforcement) unlike the bulk sample in plateau regime. By simulating reinforced foams, it was demonstrated that mechanical properties of the foams including Young modulus and tensile strength are improved considerably. Both recoverable and unrecoverable energies per unit volume in all of the compression experiments were computed and it was shown that reinforcement of foams could result in a lighter structure with improved energy absorption capability when compared to bulk polymer.

References

[1] Goren K, Chen L.M., Schadler L.S., Ozisik R., 2010, Influence of nanoparticle surface chemistry and size on supercritical carbon dioxide processed nanocomposite foam morphology, Journal of Supercritical Fluids 51: 420-427.

[2] Lee L.J., Zeng C.C., Cao X., Han X.M., Shen J., Xu G.J., 2005, Polymer nanocomposite foams, Composites Science and Technology 65: 2344-2363.

[3] Huang Y.L., Yuen S.M., Ma C.C.M., Chuang C.Y., Yu K.C., Teng C.C., Tien H.W., Chiu Y.C., Wu S.Y., Liao S., Weng F.B., 2009, Morphological, electrical, electromagnetic interference (EMI) shielding, and tribological properties of functionalized multi-walled carbon nanotube/poly methyl methacrylate (PMMA) composites, Composites Science and Technology 69: 1991-1996.

[4] Gates T., Odegard G., Frankland S., Clancy T., 2005, Computational materials: multiscale modeling and simulation of nanostructured materials, Composites Science and Technology 65: 2416-2434.

[5] Arash B., Wang Q., Varadan V., 2014, Mechanical properties of carbon nanotube/polymer composites, Scientific Reports 4: 6479.

[6] Silani M., Talebi H., Ziaei-Rad S., Kerfriden P., Bordas S.P., Rabczuk T., 2014, Stochastic modelling of clay/epoxy nanocomposites, Composite Structures 118: 241-249.

[7] Zhang Y., Zhao J., Wei N., Jiang J., Gong Y., Rabczuk T., 2013, Effects of the dispersion of polymer wrapped two neighbouring single walled carbon nanotubes (SWNTs) on nanoengineering load transfer, Composites Part B: Engineering 45: 1714-1721.

[8] Zhang Z., Liu B., Huang Y., Hwang K., Gao H., 1998, Mechanical properties of unidirectional nanocomposites with non-uniformly or randomly staggered platelet distribution, Journal of the Mechanics and Physics of Solids 58: 1646-1660.

[9] Rudd R.E., Broughton J.Q., 1998, Coarse-grained molecular dynamics and the atomic limit of finite elements, Physical Review B 58: 5893-5896.

[10] Arash B., Park H.S., Rabczuk T., 2015, Mechanical properties of carbon nanotube reinforced polymer nanocomposites: A coarse-grained model, Composites Part B: Engineering 80: 92-100.

[11] Arash B., Park H.S., Rabczuk T., 2015, Tensile fracture behavior of short carbon nanotube reinforced polymer composites: A coarse-grained model, Composite Structures 134: 981-988.

[12] Arash B., Park H.S., Rabczuk T., 2016, Coarse-grained model of the J-integral of carbon nanotube reinforced polymer Composites, Carbon 96: 1084-1092.

[13] Mousavi A.A., Arash B., Zhuang X., Rabczuk T., 2016, A coarse-grained model for the elastic properties of cross linked short carbon nanotube/polymer composites, Composites Part B: Engineering 95: 404-411.

[14] Lin F., Xiang Y., Shen H.S., 2017, Temperature dependent mechanical properties of graphene reinforced polymer nanocomposites – A molecular dynamics simulation, Composites Part B: Engineering 111: 261-269.

[15] Lin F., Yang C., Zeng Q.H., Xiang Y., 2018, Morphological and mechanical properties of graphene-reinforced PMMA nanocomposites using a multiscale analysis, Computational Materials Science 150: 107-120.

[16] Mohammadi M., Davoodi J., Javanbakht M., Rezaei H., 2017, Glass transition temperature of PMMA/modified alumina nanocomposites: Molecular dynamic study, arXiv:1803.00061v1 [cond-mat.mat-sci].
[17] Mohammadi M., Davoodi J., Thermal diffusivity of PMMA/Alumina Nano Composites Using Molecular Dynamic Simulation, arXiv:1710.01540v1 [physics.comp-ph].
[18] Alian A.R., Dewapriya M.A.N., Meguid S.A., Molecular dynamics study of the reinforcement effect of graphene in multilayered polymer nanocomposites, Materials & Design 124: 47-57.
[19] Sun R., Li L., Feng C., Kitipornchai S., Yang J., Tensile behavior of polymer nanocomposite reinforced with graphene containing defects, European Polymer Journal 98: 475-482.
[20] Shen J., Li X., Zhang L., Lin X., Li H., Shen X., Ganesan V., Liu J., Mechanical and Viscoelastic Properties of Polymer-Grafted Nanorod Composites from Molecular Dynamics Simulation, Macromolecules 51: 2641-2652.
[21] Duchaineau M.A., Elliot J.B., Hamza A.V., Dittrich T., Diaz de la Rubia T., Abraham F.F., 2011, Compaction dynamics of metallic nano-foams: A molecular dynamics simulation study, arXiv preprint arXiv:1102.3718v1.
[22] Duchaineau M.A., Hamza A.V., Diaz de la Rubia T., Abraham F.F., 2008, Atomistic simulation of compression wave propagation in nanoporous materials, arXiv preprint arXiv:0807.1332.
[23] Giri A., 2012, Molecular Dynamics Simulations of the Mechanical Deformation of Nanoporous Gold, Bachelor's Thesis, University of Pittsburgh, Pittsburgh, PA, USA.
[24] Giri A., Tao J., Wang L., Kirca M., To A.C., 2014, Compressive behavior and deformation mechanism of nanoporous open-cell foam with ultrathin ligaments, Journal of Nanomechanics and Micromechanics A4013012.
[25] Xia R., Wu R.N., Liu Y.L., Sun X.Y., 2015, The Role of Computer Simulation in Nanoporous Metals-A Review, Materials 8: 5060-5083.
[26] Plimpton S., Crozier P., Thompson A., 2007, LAMMPS-large-scale atomic/molecular massively parallel simulator, Sandia National Laboratories.
[27] Jewett A., Moltemplate, http://www.moltemplate.org/index.html.
[28] Polyak B.T., 1969, The conjugate gradient method in extremal problems, USSR Computational Mathematics and Mathematical Physics 9: 94-112.
[29] Han Y., Elliott J., 2007, Molecular dynamics simulations of the elastic properties of polymer/carbon nanotube composites, Computational Materials Science 39: 315-323.
[30] Plimpton S., 2005, LAMMPS User's Manual, Sandia National Lab.
[31] Greaves G.N., Greer A.L., Lakes R.S., Rouxel T., 2011, Poisson's ratio and modern materials, Nature materials 10: 823-837.